



Mix-mode energy management strategy and battery sizing for economic operation of grid-tied microgrid

DOI:

[10.1016/j.energy.2016.11.018](https://doi.org/10.1016/j.energy.2016.11.018)

Document Version

Accepted author manuscript

[Link to publication record in Manchester Research Explorer](#)

Citation for published version (APA):

Sukumar, S., Mokhlis, H., Mekhilef, S., Naidu, K., & Karimi, M. (2017). Mix-mode energy management strategy and battery sizing for economic operation of grid-tied microgrid. *Energy*, 118, 1322-1333. <https://doi.org/10.1016/j.energy.2016.11.018>

Published in:

Energy

Citing this paper

Please note that where the full-text provided on Manchester Research Explorer is the Author Accepted Manuscript or Proof version this may differ from the final Published version. If citing, it is advised that you check and use the publisher's definitive version.

General rights

Copyright and moral rights for the publications made accessible in the Research Explorer are retained by the authors and/or other copyright owners and it is a condition of accessing publications that users recognise and abide by the legal requirements associated with these rights.

Takedown policy

If you believe that this document breaches copyright please refer to the University of Manchester's Takedown Procedures [<http://man.ac.uk/04Y6Bo>] or contact uml.scholarlycommunications@manchester.ac.uk providing relevant details, so we can investigate your claim.



Mix-Mode Energy Management Strategy and Battery Sizing for Economic Operation of Grid-Tied Microgrid

Shivashankar.S^a Hazlie Mokhlis^{a,*} Saad Mekhilef^a K.Naidu^a M.Karimi^b

* Corresponding author at: Department of Electrical Engineering, Faculty of Engineering,
University of Malaya, 50603 Kuala Lumpur, Malaysia. Tel.: +60 3 79675238; fax: +60 3
79675316. E-mail Address: hazli@um.edu.my

^a Department of Electrical Engineering, University of Malaya, 50603 Kuala Lumpur,
Malaysia

^b School of Electrical and Electronics Engineering, The University of Manchester, United
Kingdom

Abstract

This paper presents a novel ‘mix-mode’ energy management strategy (MM-EMS) and its appropriate battery sizing method for operating the microgrid at the lowest possible operating cost. The MM-EMS is developed by combining three proposed operating strategies, namely “continuous run mode”, “power sharing mode” and “ON/OFF mode” for a 24h time period. The objective functions for the proposed strategies are solved using linear programming (LP) and mixed integer linear programming (MILP) optimization methods. A sizing method using the particle swarm optimization (PSO) technique to determine the optimal energy capacity of battery energy storage (BES) in kWh is also presented. Since the size of the BES influences the microgrid’s operating cost, the energy management strategy (EMS) and BES capacity are simultaneously optimized. The proposed MM-EMS and battery sizing method were first validated. Then, the variation of optimal battery capacity for different battery state of charge (SOC) levels is analyzed. The variation of microgrid’s associated costs for different battery’s

25 initial state of charge (SOC) levels is analyzed as well. Finally, a recommendation on the choice
26 of initial SOC level during the start of the day for the economic operation of microgrid is also
27 suggested.

28 **Keywords**

29 Energy management, battery storage, battery sizing, microgrids and particle swarm optimization
30 (PSO).

31 **1. Introduction**

32 The conventional power system distribution network is currently undergoing a major change due
33 to the addition of microgrids. The benefits of using microgrids include the fact that it is capable
34 of supplying loads with negligible losses, reduce fossil fuel consumption, and postpone
35 investment in a distribution system. Connecting intermittent sources such as solar photovoltaic
36 (PV) generators and wind turbines in the grid-connected microgrid introduces challenges in
37 various technical aspects, such as power quality, protection, generation dispatch control, and
38 reliability. Challenges caused by these intermittent sources render the battery energy storage
39 (BES) an indispensable source [1]. When a grid connected microgrid consists of two or more
40 dispatchable source, it is necessary for the grid operator to run it economically. If battery energy
41 storage (BES) is one of the dispatchable sources, it is essential that an appropriate size of BES is
42 installed for the optimal microgrid operation.

43 A power management and battery sizing algorithm is proposed for a grid connected microgrid,
44 consisting of PV, diesel generator, and BES in [2]. However, the battery size is not optimum,
45 because the algorithm does not consider economic operation of microgrid. A smart energy
46 management system based on matrix real-coded genetic algorithm is proposed in [3] for
47 economic operation of grid connected microgrid. The optimal operation of grid connected

48 microgrid is presented in [4,5], where the microgrid's economic dispatch problem is solved by
49 minimizing the microgrid's operational cost using mesh adaptive direct search (MADS)
50 algorithm. Mixed integer linear programming (MILP) is used to solve the economic dispatch of
51 microgrid sources in [6]. An optimal energy management is presented in [7], where the objective
52 is to minimize the generation cost of the grid connected microgrid. The economic dispatch
53 problem is solved using mixed integer quadratic programming (MIQP). Similarly, the sizing of
54 battery energy storage is carried out in [8], where the economic dispatch problem is solved using
55 linear programming (LP). Apart from solving the energy management problem using numerical
56 methods, metaheuristic methods are used to solve energy management problem found in [9-12].
57 The energy management problem from the aforementioned references is based on one particular
58 strategy. Moreover, in few papers, the optimal sizing of battery storage is not taken into account.
59 Energy storage devices play a crucial role in the economic operation of microgrid. Battery
60 storage can take advantage of time of use tariffs, where it can be an effective option when the
61 power purchasing price from the utility grid is high. Therefore, the accurate sizing of battery
62 source is essential to ensure a microgrid's economic operation. The sizing of BES involves
63 determining the optimal energy capacity in kWh with the aim of reducing microgrid's daily
64 operating cost. An optimal sizing of battery storage for microgrid is presented in [13]. The
65 optimal sizing of battery energy storage using improved bat algorithm is presented in [14].
66 Genetic algorithm based method for sizing battery storage is proposed in [15]. The energy
67 management system in this paper is based on fuzzy expert system. In [16], matrix real-coded
68 genetic algorithm (MRCGA) is used to determine the optimal energy capacity of BES. In a
69 recently published article [17], the battery size is evaluated in order to minimize the microgrid's
70 operation cost. The sizing problem was solved using Grey Wolf Optimizer (GWO). The energy

71 management problem solved in aforementioned references is based on a single operating
72 strategy. The battery sizing methods presented in these references is focused on one particular
73 energy management strategy, which may not incur the lowest operating cost.

74 The prominent focus of most work in literature pertaining to this subject was on solving
75 economic dispatch for microgrid sources using a single operating strategy. It is possible that the
76 microgrid might operate at lower operating cost in the case of a newly designed operating
77 strategy. There are only a few works in literature that accounted for the sizing of battery storage,
78 which is an important aspect of economic operation of a microgrid. In addition the papers in the
79 literature discuss battery sizing methods that considers the economic operation of microgrid for
80 one particular strategy. Therefore, in this paper an energy management strategy to operate the
81 grid connected microgrid at the lowest possible operating cost is discussed. A method to estimate
82 optimal BES size in kWh will also be presented. This work involves the development of an
83 energy management using mix-mode operating strategy to operate the microgrid at the lowest
84 possible operating cost. The proposed mix-mode operating strategy is developed by combining
85 three proposed operating strategies, namely “continuous run mode”, “power sharing mode” and
86 “ON/OFF mode” for a 24h time period. The objective functions for these operating strategies
87 were minimized using linear programming (LP) and mixed integer linear programming (MILP)
88 methods. The mix-mode operating strategy is based on combining the aforementioned strategies
89 keeping the operating cost in mind. The non-linearity of the PV output power and load demand,
90 daily grid electricity price profile, the price of the natural gas, as well as battery state of charge
91 (SOC) limits were all taken into account in the development of this model. In this paper, the
92 BES’s energy capacity for the microgrid under the proposed mix-mode operating strategy is
93 solved using the PSO optimization technique. Due to the fact that the operating cost produced

94 using mix-mode strategy depends on the characteristics of battery storage, both the EMS and
95 BES capacity needs to be simultaneously optimized. The discussion section will detail the,
96 validation of the proposed MM-EMS and battery sizing method. Then, the variation of the
97 optimal battery capacity for different battery state of charge (SOC) level is analyzed. Also, an
98 analysis on variation of microgrid's operating cost (OC), battery's total cost per day (TCPD), and
99 the combined cost of OC and TCPD will be carried out for different values of initial SOC levels.
100 Finally, a recommendation is also suggested on choice of battery's initial SOC level during start
101 of the day.

102 **2. Proposed 'Mix-Mode' Energy Management Strategy (MM-EMS)**

103 Operating the microgrid in more than one operating strategy is referred to as the mix-mode
104 operating strategy. Three operating strategies, namely the continuous run mode, power sharing
105 mode, and ON/OFF mode are proposed and explained in the following subsections.

106 **2.1 Proposed operating strategies**

107 The optimal generation dispatch for energy sources is calculated on an hourly basis to satisfy the
108 load requirements considering hybrid system limits and constraints. The proposed operating
109 strategies are explained in the subsequent sections.

110 **2.1.1 Strategy 1: Continuous run mode**

111 In this operating mode, the power drawn from the utility grid is always zero. The fuel cell
112 operates continuously during a 24h time period. The output power from the fuel cell depends on
113 the load demand and output powers from the PV and battery storage. During this strategy,
114 initially the output power from PV and battery is used to supply the load demand. If demand is
115 not met, the fuel cell is optimally dispatched to satisfy the load demand. There are chances where
116 the output power from the PV exceeds the load demand, and in this case, the battery is charged,

117 and the fuel cell is forcibly switched OFF. The objective function for this mode is to reduce the
 118 daily operating cost, which can be expressed as:

$$119 \quad obj1 = \text{Minimize} \left[C_{gi} \sum_{i=1}^N \frac{P_{FCi}}{\eta_i} + \beta(P_{BATi}) \right] \quad (1)$$

120 where,

121 C_{gi} is natural gas price to supply the fuel cell in dollars per kilowatt-hour

122 P_{FCi} is fuel cell power at time interval 'i'

123 β is taken as 1×10^{-6} to obtain the dispatch solution of P_{BATi}

124 P_{BATi} battery power at time interval 'i';

125 If P_{BATi} is positive battery discharges mode, if P_{BATi} is negative battery charging mode

126 η_i is cell efficiency of SOFC at time interval 'i' which is given as,

$$127 \quad \eta_i = \frac{\left(\frac{V_{stack(i)}}{N} \right)}{E^o} \quad (2)$$

128 E^o is standard electrochemical potential which is 1.482 volt/cell

129 V_{stack} is fuel cell output stack voltage at instant 'i'

130 N is number of cell in fuel cell stack

131 At any given time instant 'i', the sum of the power generated from the distributed sources should
 132 be equal to the load, which can be expressed as:

$$133 \quad P_{PVi} + P_{BATi} + P_{FCi} = P_{Li} \quad i = 1, 2, \dots, 24 \quad (3)$$

134 The power produced from PV is uncontrollable. The fuel cell and battery is modeled as a
 135 variable controllable source, which should be operated within the prescribed limits for a 24h time
 136 period. The constraints for the controllable source are given as:

137
$$P_{FC\min} \leq P_{FCi} \leq P_{FC\max} \quad i = 1,2,\dots,24 \quad (4)$$

138 The constraints related to battery energy level and allowable charge/discharge power considered
 139 for this work will be explained in Section 3.

140 **2.1.2 Strategy 2: Power sharing mode**

141 In this power sharing mode, the utility grid, battery source, and fuel cell are all optimally
 142 scheduled to supply power to the load demand. The battery source is charged when the output
 143 power from the PV exceeds that of the load demand. The objective function for the power
 144 sharing mode is to reduce the daily operating cost, which can be expressed as:

145
$$obj2 = \text{Minimize} \left[C_{gi} \sum_{i=1}^N \frac{P_{FCi}}{\eta_i} + C_{ei} (P_{Li} - P_{neti}) + \beta (P_{BATi}) \right] \quad (5)$$

146 where,

147 C_{ei} tariff of electricity purchased in dollar per kilowatt-hour

148 P_{Li} is the load demand at interval ‘ i ’

149 P_{neti} is the net power produced at interval ‘ i ’

150 At any instant of time ‘ t ’, the summation of total generated power from PV, fuel cell, battery
 151 source and utility grid should be equal to the total load demand.

152
$$P_{PVi} + P_{BATi} + P_{FCi} + P_{Gi} = P_{Li} \quad i = 1,2,\dots,24 \quad (6)$$

153 Since the microgrid operates at the distribution level, the excess power from the microgrid is
 154 utilized to charge the battery. This is necessary to avoid the power from being injected to grid,
 155 which will activate the reverse power flow relay installed at the point of common coupling
 156 (PCC). The power imported from the grid at time instant ‘ i ’ can be used to charge the battery or

157 supply the load. Therefore, considering the power drawn from the grid as a constraint which can
 158 be expressed as,

$$159 \quad P_{Gi} \geq 0 \quad i = 1,2,\dots,24 \quad (7)$$

160 Moreover, the boundary constraints for fuel cell given in eq.(4) are taken into account for this
 161 strategy. The limitations related to battery energy level and allowable charge/discharge power
 162 considered for this work will be explained in Section 3.

163 **2.1.3 Strategy 3: ON/OFF mode**

164 In this strategy, the objective is to obtain an optimal ON/OFF schedule for the fuel cell, utility
 165 grid, and battery source, thereby minimizing the microgrid's operating cost. Here, the output
 166 power from both the PV and battery source supplies the load demand. Any deficit in the power
 167 required by the load is delivered by optimally dispatching fuel cell and the utility grid. In this
 168 operating strategy, when the fuel cell is switched ON, it is forced to run at its rated output power.
 169 For the rest of the time, the fuel cell is switched OFF. Since the fuel cell is switched ON/OFF, a
 170 binary switching variable is introduced to enhance control over the fuel cell. The objective
 171 function for this ON/OFF mode is given as:

$$172 \quad obj3 = Minimize \left[S(i) \left(C_{gi} \sum_{i=1}^N \frac{P_{FCi}}{\eta_i} \right) + C_{ei} (P_{Li} - P_{neti}) + \beta (P_{BATi}) \right] \quad (8)$$

173 Where $S(i)$ is a switching function, which takes the value of 0 or 1. When $S(i)$ is 1, the fuel cell is
 174 operated at its rated capacity. When $S(i)$ is 0, the fuel cell is switched OFF. Therefore, during the
 175 time of the fuel cell operation, its output is constant.

176 At any given time instant 'i', the sum of power generated from the distributed sources and utility
 177 grid should be equal to the load, which can be expressed as:

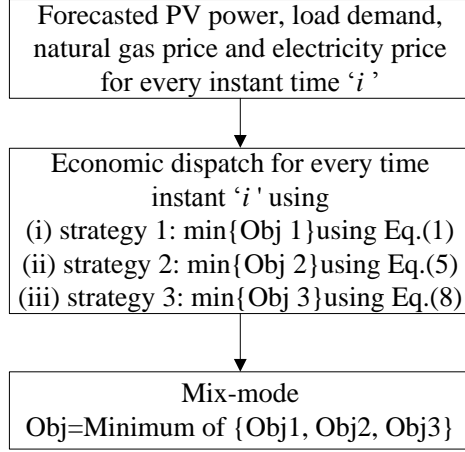
178
$$P_{PVi} + P_{BATi} + (P_{FCi})S(i) + P_{Gi} = P_{Li} \quad i = 1,2,\dots,24 \quad (9)$$

179 Since the fuel cell is forced to run at its rated capacity, the operating range of fuel cell is either
180 zero or at its rated capacity. The boundary constraint for utility grid power eq.(7) is also
181 considered. The limitations related to battery energy level and allowable charge/discharge power
182 considered for this work will be explained Section 3.

183 **2.2 Development of mix-mode operating strategy**

184 This section explains the development of “*mix-mode*” operating strategy. The primary objective
185 of mix-mode operating strategy is to dispatch power from the distributed sources to the varying
186 load with lower daily operating cost. The idea of mix-mode strategy is presented in Fig. 1.
187 Initially the forecasted PV output power and load demand for the time instant ‘*i*’ is considered.
188 For the given time instant with the PV power, load demand, prices of electricity and natural gas
189 as inputs, the economic dispatch problem is solved for the three proposed strategies. *Obj1*, *Obj2*,
190 and *Obj3* are the obtained objective functions for strategy 1, strategy 2 and strategy 3,
191 respectively, for the given time instant ‘*i*’. The lowest value of the three objective functions
192 should deliver the lowest operating cost. Therefore, the optimal dispatch values corresponding to
193 the lowest objective function is selected and provided as a reference to the distributed generators
194 present in the microgrid. The aforementioned steps are repeated for every time instant ‘*i*’ and this
195 microgrid is operated for 24h time period.

196



197

198

Fig.1. Mix-mode operating strategy

199

3. Optimal sizing of battery source for MM-EMS: Problem formulation

200

On top of the proposed energy management strategy, optimal sizing of BES for MM-EMS is also

201

formulated. To obtain the optimal battery sizing, the initial capital cost (CC) of BES should be

202

considered. Total cost per day for BES ($TCPD_{BAT}$) is the function of initial capital cost of BES.

203

The optimal BES sizing is obtained by minimizing the total cost function, which is a summation

204

of the daily operating cost of microgrid and BES's $TCPD_{BAT}$. The daily operating cost of the

205

microgrid (Obj) is obtained from the previous section by operating the microgrid in the mix-

206

mode operating strategy. Therefore, the total cost function formulated for this problem can be

207

given as:

208

$$MinF(X) = \sum_{i=1}^{24} Obj(i) + TCPD_{BAT} \quad (10)$$

209

Here, the $TCPD_{BAT}$ for a particular battery energy rating will be same for all the three strategies.

210

The expression for $TCPD_{BAT}$ is given as,

211

$$TCPD_{BAT} = \frac{1}{365} \left(\frac{r.(1+r)^{Lt}}{(1+r)^{Lt} - 1} . CC \right) \quad (11)$$

212

$$CC = C_P . \bar{P} + C_E . \bar{E} \quad (12)$$

213 where CC is the capital cost of the battery source, and C_P and C_E are specific costs associated
 214 with the battery source's power and energy capacities, respectively. r is interest rate for financing
 215 the battery source, Lt is the battery source's lifetime and \bar{E} and \bar{P} are rated energy and power
 216 capacities of the BES.

217 The proposed sizing problem is solved subjected to constraint given below,

218 **(a) Battery constraints:**

219 The charge in the BES must be bounded between,

$$220 \quad E_{BAT}^{\min} \leq E_{BAT} \leq E_{BAT}^{\max} \quad (13)$$

221 where E_{BAT} is the energy stored in the battery at the end of instant 'i' in kWh.

222 E_{BAT}^{\min} , E_{BAT}^{\max} are minimum and maximum charges to be maintained for battery storage

223 **Discharging mode:**

224 Constraint limited to release of energy from battery source is given as,

$$225 \quad E_{BAT,i} = \max \left\{ \left(E_{BAT,i-1} - \Delta t \cdot P_{BAT,i} / \eta_{discharge} \right), E_{BAT}^{\min} \right\} \quad (14)$$

226 **Charging mode:**

227 Constraint limited to energy stored in the battery source is given as,

$$228 \quad E_{BAT,i} = \min \left\{ \left(E_{BAT,i-1} + \Delta t \cdot P_{BAT,i} \cdot \eta_{charge} \right), E_{BAT}^{\max} \right\} \quad (15)$$

229 In addition to the limitation in charging/discharging levels, the maximum and minimum
 230 discharging/charging power is also given as,

$$231 \quad P^c_{BAT,i} \leq P_{BAT,i} \leq P^d_{BAT,i} \quad i = 1, 2, \dots, N \quad (16)$$

232 where,

$$233 \quad P^c_{BAT,i} = \max \left\{ P_{BAT,\min}, \left(E_{BAT,i-1} - E_{BAT}^{\max} \right) / \eta_{charge} \cdot \Delta t \right\} \quad i = 1, 2, \dots, N \quad (17)$$

$$234 \quad P^d_{BAT,i} = \min \left\{ P_{BAT,\max}, \left(E_{BAT,i-1} - E_{BAT}^{\min} \right) \eta_{discharge} / \Delta t \right\} \quad i = 1, 2, \dots, N \quad (18)$$

235 Δt is the commitment period which is 1h in this paper

236 The proposed battery sizing problem should fulfill the aforementioned constraints in Eq.(13)-
237 (18) for solving the energy management strategy proposed in Section 2.

238 **(b) Dispatchable distributed generator constraints**

239 The PV source is uncontrollable, and its output depends on solar radiation. The operating output
240 of other dispatchable sources should be limited within the minimum and maximum limits. The
241 operating limits of the fuel cell and utility grid for the proposed strategies are provided in
242 corresponding Sections 2.1.1, 2.1.2, 2.1.3.

243 **4. Proposed sizing method**

244 In the ordinary form, solving the optimal BES sizing for the proposed mix-mode operating
245 strategy is a complex optimization problem. Therefore, the particle swarm optimization (PSO)
246 technique, which is a population based optimization technique, is used to solve the battery sizing
247 problem. The economic dispatch problems proposed in the three strategies are solved using
248 linear programming (LP) and mixed-integer linear programming (MILP) optimization
249 techniques. The objective functions for the strategy 1 and strategy 2 for continuous run and
250 power sharing modes have been modeled as a linear function of microgrid's distributed sources
251 output power. Therefore, for strategy 1 and strategy 2, the optimization problem is solved using
252 the linear programming (LP) solver “*linprog*” in MATLAB, which can be expressed as:

$$253 \quad \min_x f^T obj \text{ subjected to } \begin{cases} A.x \leq b \\ Aeq.x = beq \\ lb \leq x \leq ub \end{cases} \quad (19)$$

254 where: f , x , b , beq , lb and ub are vectors; A and Aeq are matrices.

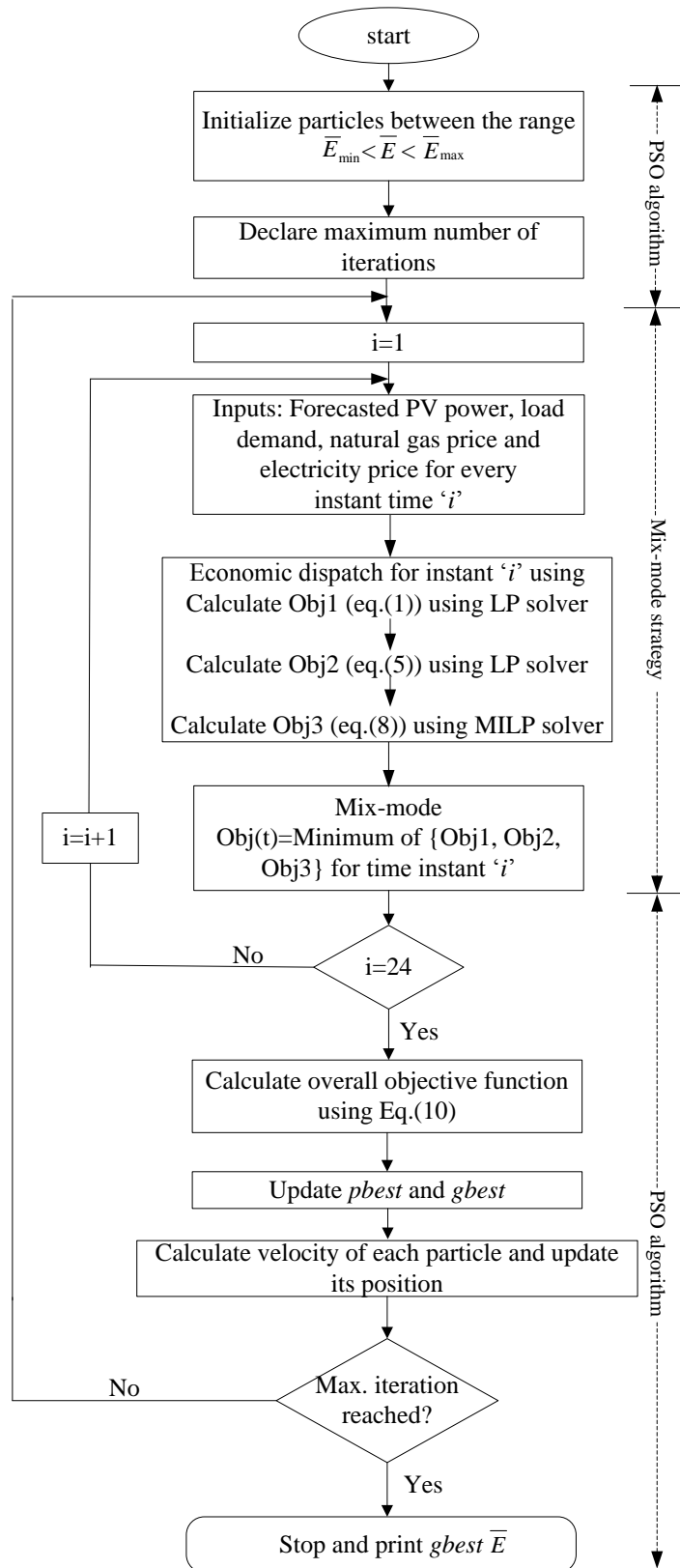
255 The objective function for strategy 3 has been modeled as a mixed integer linear function of the
 256 microgrid's distributed sources output power, where the switching function for the fuel cell
 257 generator in Eq.(8) is an integer. Therefore, the objective function is modeled as a mixed integer
 258 linear programming (MILP). This MILP problem can be solved using MILP solver “*intlinprog*”
 259 in MATLAB. The “*intlinprog*” finds minimum of a problem by considering the constraints
 260 specified by,

$$261 \quad \min_x f^T obj \text{ subjected to } \begin{cases} x(int\ con) \\ A.x \leq b \\ A_{eq}.x = b_{eq} \\ l_b \leq x \leq u_b \end{cases} \quad (20)$$

262 where: f , x , $intcon$, b , beq , lb and ub are vectors; A and Aeq are matrices.

263 The BES's energy capacity for the microgrid under the proposed mix-mode operating strategy is
 264 solved using PSO. Simultaneously, the economic dispatches for three strategies are performed
 265 using linear programming and mixed-integer linear programming optimization techniques. In
 266 support of this, the flowchart of the proposed battery sizing method is presented in Fig.2.

267



268

269

Fig. 2. Flowchart of the proposed sizing method for mix-mode energy management strategy

270 The proposed methodology is based on 24h microgrid operation. To perform the sizing of battery
271 source, 24h data for the following variables are required: forecasted PV output power, load
272 demand, natural gas price and utility grid electricity price. As the first step in the proposed
273 method, the particles between the range is declared to be,

$$274 \quad \bar{E}_{\min} < \bar{E} < \bar{E}_{\max} \quad (21)$$

275 The value of \bar{E}_{\min} and \bar{E}_{\max} is set according to the microgrid's characteristics. In this paper, the
276 value of \bar{E}_{\min} and \bar{E}_{\max} is set as 100 kWh and 3,000 kWh, respectively. It means that the search
277 space for PSO is between the range of [100 kWh, 3,000 kWh]. The power capacity of the battery
278 \bar{P} is fixed to 100 kW in this paper. Initially, particles between the search ranges are generated
279 randomly. Then, for each particle, the economic dispatch is solved for every time instant 't' for
280 the three proposed operating strategies. The operational constraint for the battery source, fuel
281 cell, and utility grid is considered while solving the economic dispatch problem. From the three
282 solved objective function for time instant 't', the lowest objective function is selected and
283 explained in Section 2.2. This procedure is repeated for the 24h time period. Then the objective
284 function (*Obj*) for a 24h time period solved using mix-mode strategy is summed with the
285 $TCPD_{BAT}$ to obtain the overall cost function. This procedure is repeated for all of the particles.
286 Once the objective functions for all the particles are evaluated, the particles personal best (*pbest*)
287 and global best (*gbest*) is updated. Then, the velocity of each particle is updated, and based on
288 the velocity, the new position of the particles is obtained. Thus, the whole process is repeated
289 until the maximum number of iterations is reached. When the number of iteration reaches its
290 maximum, the system prints the optimal value of BES capacity \bar{E} in kWh.

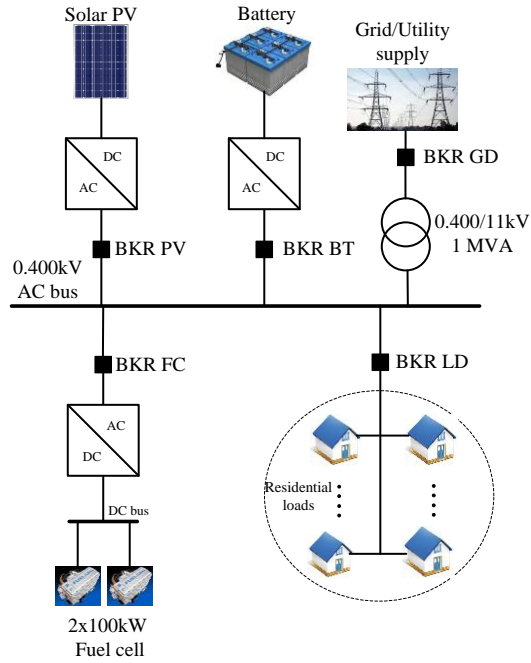
291

292

293 5. Case studies and results discussion

294 To assess the validity of the proposed mix-mode energy management strategy and the proposed
295 battery sizing method, a low voltage grid connected microgrid shown in Fig. 3 is considered. The
296 grid connected microgrid consists of 200 kW solar PV, two identical 100 kW solid oxide fuel
297 cell, and a battery bank operated parallel with the load. The minimum and maximum operating
298 range of the single fuel cell unit is fixed as 10 kW and 100 kW, respectively. Operating outside
299 the operating range will reduce the fuel cell's life [18]. The technical specification considered for
300 modeling solid oxide fuel cell is taken from [19]. Utility grid electricity pricing and natural gas
301 pricing is shown in Fig.4 and is obtained from [20]. The forecasted PV output power and load
302 demand for 24h time horizon is considered for this work. The microgrid uses lead-acid battery,
303 while the specific costs associated with the BES's power capacity (C_P) and energy capacity (C_E)
304 are set as \$234/kW and \$167/kWh, respectively [15]. The battery lifetime and interest rate for
305 financing the battery source are set as 3 yrs and 6%, respectively. The charging and discharge
306 efficiency are same and are set to 95%. $P_{BAT,min}$ and $P_{BAT,max}$ of the battery is set as -100 kW and
307 100 kW, respectively. The minimum and maximum level of SOC for the battery should be
308 maintained within 20% and 100%, respectively. To reflect this in the optimization, E_{BAT}^{min} and
309 E_{BAT}^{max} are minimum and maximum level of charge that should be maintained, which is set as 20%
310 of \bar{E} and 100% of \bar{E} , respectively.

311 As a first step the superiority of the proposed mix-mode operating strategy in reducing the
312 overall microgrid's operating cost for a particular battery capacity is presented. Then, the
313 proposed battery sizing method is validated by comparing it to the trade-off method. The
314 variation of the optimal battery sizes for different battery's initial SOC levels is presented. With
315 this, an analysis on variation in microgrid's operating cost is also carried out.

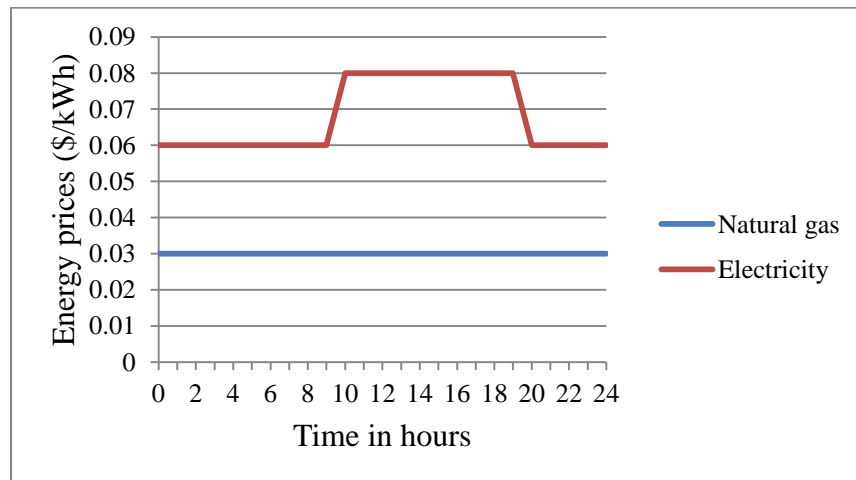


316

317

318

Fig.3 Microgrid test system



319

320

321

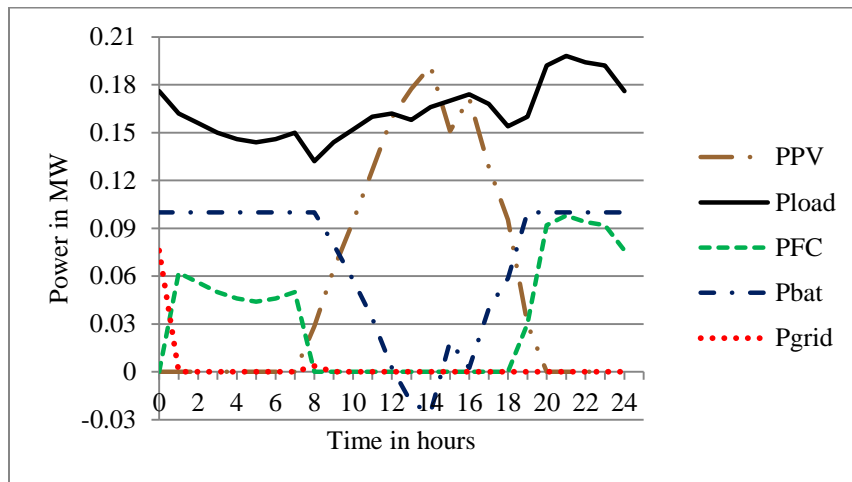
322

323

Fig.4. Utility energy prices in (\$/kWh)

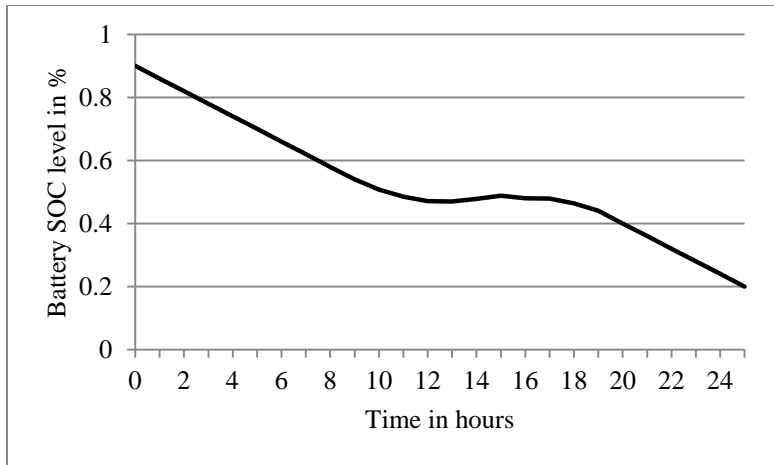
324 **5.1 Comparison of the proposed mix-mode operating strategy with other operating**
325 **strategies**

326 In this section, the superiority of the proposed mix-mode energy management strategy is
327 validated for the microgrid model presented in Fig. 3. In this study, since the battery source is
328 considered, the optimal size of the battery is determined using the proposed sizing method. The
329 initial SOC level of the battery during the start of the day is kept at 90%. The battery size is
330 optimized within the range [100 kWh, 3,000 kWh], considering all the battery and distributed
331 sources constraint. The optimal battery capacity for this case is found to be 2,497.6 kWh. The
332 results of the optimal dispatch values for the distributed sources in the microgrid for mix-mode
333 strategy are presented in Fig. 5. Fig. 6 show the battery state of charge (SOC) level maintained
334 within its limit.



335
336 Fig.5. Optimal output of distributed source in microgrid for mix-mode strategy

337



338

339

Fig.6. Battery SOC level for mix-mode operating strategy

340

341 A comparison on the daily operating cost for the proposed mix-mode strategy with other

342 strategies is tabulated in Table 1.

343

Table 1 Comparison of daily operating cost

| | Strategy 1: Continuous run mode | Strategy 2: Power sharing mode | Strategy 3: ON/OFF mode | Mix-mode |
|----------------------------|---------------------------------------|--------------------------------------|-------------------------------|----------|
| Operating cost in \$ | 1,880.8 | 1,003.5 | 1,073.6 | 978.8768 |
| FC operating hours | 24 | 14 | 4 | 13 |
| Grid operating hours | 0 | 1 | 11 | 2 |

344

345 The results from Table 1 shows that operating the microgrid in continuous run mode is more

346 expensive. The fuel cell is also forced to run for the 24h time period. The operating cost of

347 microgrid is found to be less when the microgrid is operated under the power sharing mode when

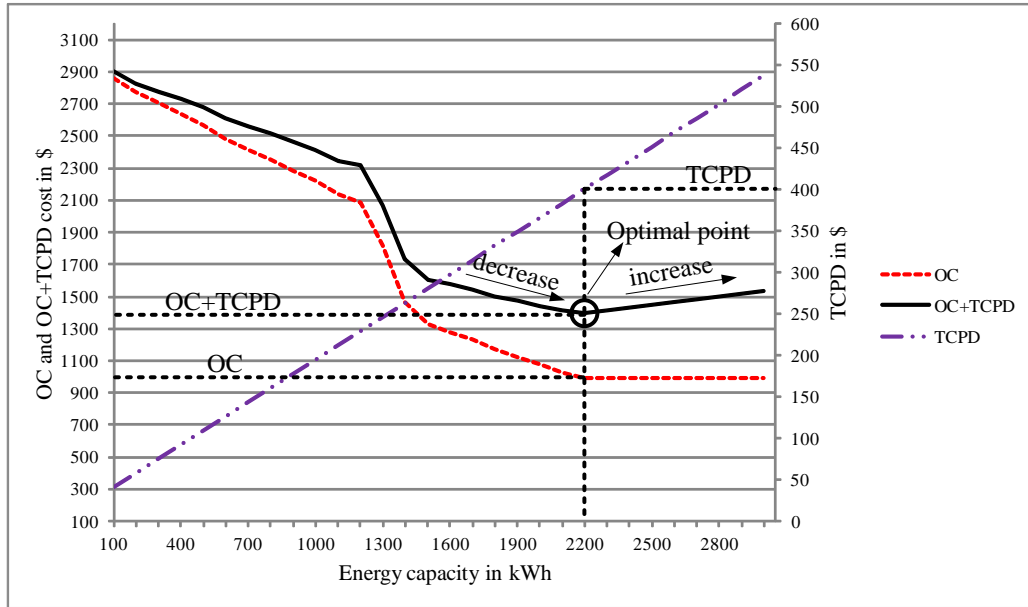
348 compared to the ON/OFF mode. However, the fuel cell is operated for 14h, which exceeded the

349 ON/OFF mode where the fuel cell is forced to run at its rated capacity for only 4h. The

350 advantage of operating the microgrid in the ON/OFF mode is that, when the fuel cell is forced to
351 run at the ON/OFF mode, the excess power can be used to charge the battery source. Moreover,
352 the run time of fuel cell is less during the ON/OFF mode, which will increase its calendar life.
353 The overall operating cost of the microgrid for the proposed mix-mode operating strategy is less
354 than other operating strategies. This proves that operating a microgrid in different operating
355 strategies for 24h time period will incur the lowest operating cost.

356 **5.2 Validation of the proposed battery sizing method**

357 In this section, the validation of the proposed battery sizing method is carried out. The proposed
358 battery sizing method is validated with the “trade-off” method. Trade-off method can be used to
359 find the approximate battery storage capacity in kWh. For this purpose, the operating cost (OC)
360 of the microgrid, battery’s TCPD, and sum of OC and TCPD cost is plotted for different values
361 of the battery’s energy capacity. Since the minimum and maximum range of the battery energy
362 capacity for this work is [100 kWh , 3,000 kWh], the OC , $TCPD_{BAT}$, and $(OC+TCPD_{BAT})$ are
363 plotted in Fig.7 for different energy capacities between these ranges on regular intervals. Fig. 7 is
364 plotted by taking into account the initial charge of the battery being equal to 100% of the battery
365 capacity, which is the initial SOC level of the battery during the start of the day taken as 100% in
366 this case.



367

368

Fig.7 Optimal value of energy capacity in kWh using trade-off method

369

The operating cost (OC) of the microgrid is very high for lower battery capacities. As the battery

370

capacity increases, the OC of the microgrid decreases. This is due to the availability of sufficient

371

battery source for an economical microgrid operation. On the other hand, as the battery capacity

372

increases, the battery's TCPD cost also increases. This is because the TCPD of the battery is

373

directly associated with battery's installation cost. Therefore, with an increase in the battery

374

capacity starting from 100 kWh, the sum of operating cost (OC) and battery's TCPD, which is

375

the combined cost of *OC* and *TCPD*, tend to decrease. With the increase in battery capacity at

376

one point, the OC of the microgrid attains a minimum value, from where it does not decrease and

377

remains constant for further increment in battery capacity. In this instant, the readers can notice a

378

sudden change from a decreasing to an increasing trend in the combined cost of *OC* and *TCPD*

379

costs. The point where a sudden change in the trend happens to be the optimal point, where the

380

combined cost *OC+TCPD* is quite less. The point where the combined cost of *OC* and *TCPD* is

381

less is encircled in Fig. 7, for which the corresponding battery capacity is found to be 2,200

382

kWh. Here, the optimal battery capacity is obtained by a trade-off between microgrid's *OC* and

383 battery's TCPD costs. The approximate operating cost (OC) of the microgrid for the optimal
384 value is plotted, and it is found to be \$ 1,000, while the TCPD cost associated with the battery is
385 approximately \$ 400. Therefore, the total combined cost of OC and TCPD from the Fig. 7 is
386 closer to \$ 1,400 per day. That is the point encircled in Fig.7, where it is closer to \$ 1,400 per
387 day. It can be noted from Fig. 7 that further increase in battery capacity beyond the 2,200 kWh
388 increases the combined cost of OC and TCPD, which is due to the increase in battery's TCPD
389 cost. On the other hand, it can be noticed that the OC of the microgrid remains constant for
390 further increase in battery capacity beyond 2,200 kWh. Choosing any value below 2,200 kWh
391 will increase the microgrid's operating cost.

392 In this paper, we propose an accurate method to determine optimal battery size using the PSO
393 optimization technique necessary for economic operation of microgrid. The microgrid is
394 operated in a mix-mode operating strategy. In this case, the battery size and operating cost of the
395 microgrid are simultaneously optimized. The battery capacity is optimized by considering the
396 initial SOC level during start of the day as 100%. The optimal value of battery capacity
397 optimized using PSO is found to be 2,185.4 kWh. Table 2 provides a comparison between the
398 optimal value of battery capacity obtained using the trade-off method and the proposed sizing
399 method. In the table, the OC, TCPD and OC+TCPD costs obtained from the proposed sizing
400 method is compared with the trade-off method. The capacity of the battery and costs tabulated
401 for the proposed sizing method is very close to the values obtained using the trade-off method.
402 From the table, it is clear that the proposed battery sizing method is accurate enough to calculate
403 the battery capacity in kWh for the economic operation of the microgrid.

404

405 Table 2 Comparison of optimal value obtained using trade-off method and proposed sizing
 406 method

| | Trade-off method | Proposed sizing method |
|--------------------------------|------------------|------------------------|
| Optimal battery capacity (kWh) | 2,200 | 2,185.4 |
| OC (\$) | 1,000 | 978.8768 |
| TCPD (\$) | 400 | 398.0547 |
| OC+TCPD (\$) | 1,400 | 1,376.9315 |

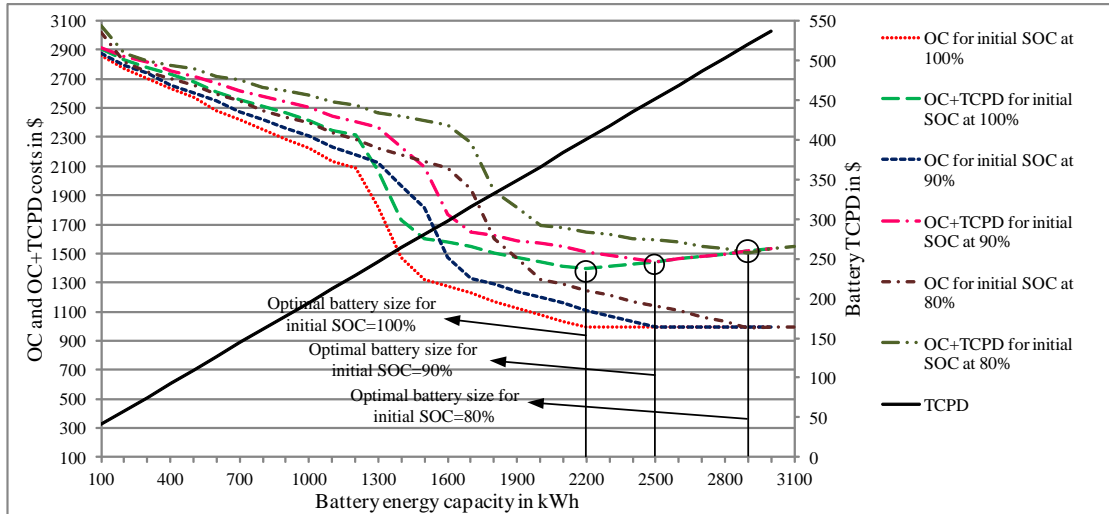
407
 408

409 **5.3 Analysis of variation in optimal energy capacity of battery source for initial SOC levels**
 410 **100%, 90% and 80% during start of the day**

411 The main advantage of adding battery source in the microgrid is to maintain stability, improve
 412 power quality, and facilitate the integration of renewable sources [21-24]. In this case, the
 413 optimal battery capacity required for the economic microgrid operation is evaluated by
 414 considering the initial SOC of the lead acid battery to be 100%, 90%, and 80% during the start of
 415 the day. Therefore, the optimal battery capacity \bar{E} for each of the initial SOC level is optimized
 416 within the range [100 kWh , 3,000 kWh] using the proposed battery sizing method.

417 The optimal values of the BES are found to be 2,185.4 kWh, 2,497.6 kWh and 2,913.9 kWh
 418 when the battery initial SOC levels are 100%, 90% and 80% respectively during the start of the
 419 day. This is validated using the trade-off method by plotting various costs against different
 420 battery capacity ranging between [100 kWh , 3,000 kWh].

421 The results for the optimal energy capacity using the trade-off method when the microgrid is
 422 operated under mix-mode strategy, considering the battery source with initial SOC levels as
 423 100%, 90% and 80% during the start of the day are presented in Fig.8. The optimal values are
 424 attained for the lowest value of combined cost of OC and TCPD is found to be 2,200 kWh, 2,500
 425 kWh and 2,900 kWh for initial SOC cases of 100%, 90%, and 80% respectively.



426

427 Fig. 8. Optimal value of energy capacity in kWh using trade-off method for initial battery SOC at
 428 100%, 90% and 80%

429 From Fig.8, it can be noted that the microgrid’s operating cost (OC) and the combined cost of
 430 OC and TCPD is not same when the battery source initial SOC levels during start of the day are
 431 100%, 90% and 80%. The OC and combined cost of OC and TCPD is very much decreased
 432 when the battery initial SOC level during the start of the day is 100%. In other words, if the
 433 battery’s initial SOC level is very large, the operating cost of the microgrid is reduced to its
 434 lowest value. Fig.8 shows that the operating cost of the microgrid settles to a constant value of
 435 the battery’s optimal capacity value. For example, in the case of the battery initial SOC level
 436 100%, the operating cost settles at an approximate value of \$ 1,000 at 2,200 kWh. Similarly, for
 437 cases of initial SOC levels at 90% and 80%, the operating cost settles down to a constant value
 438 of \$ 1,000 at optimal values of 2,500 kWh and 2,900 kWh, respectively. A clear comparison
 439 between the optimal values obtained for different battery initial SOC levels for the trade-off
 440 method and the proposed sizing method is presented in Table 3.

441

442

443 Table 3. Comparison of optimal value obtained using trade-off method and proposed sizing
 444 method for battery initial SOC levels 100%, 90% and 80%

| Initial SOC at | Trade-off method | | | Proposed sizing method | | |
|--------------------------------|------------------|-------|-------|------------------------|------------|------------|
| | 100% | 90% | 80% | 100% | 90% | 80% |
| Optimal battery capacity (kWh) | 2,200 | 2,500 | 2,900 | 2,185.4 | 2,497.6 | 2,913.9 |
| OC in \$ | 1,000 | 1,000 | 1,000 | 978.8768 | 978.8768 | 978.8768 |
| TCPD in \$ | 400 | 450 | 520 | 398.0547 | 451.4934 | 522.7506 |
| OC+TCPD in \$ | 1,400 | 1,450 | 1,520 | 1,376.9315 | 1,430.3702 | 1,501.6274 |

445
 446 Table 3 show that with decreasing levels of the battery’s initial SOC level during the start of the
 447 day, the battery’s optimal capacity increases. Therefore, in order to reduce the microgrid’s
 448 operating cost to its lowest value with less battery initial cost, it is suggested that the optimal
 449 battery capacity with higher initial SOC be used during the start of the day. This will reduce the
 450 microgrid’s operating cost with less battery initial cost.

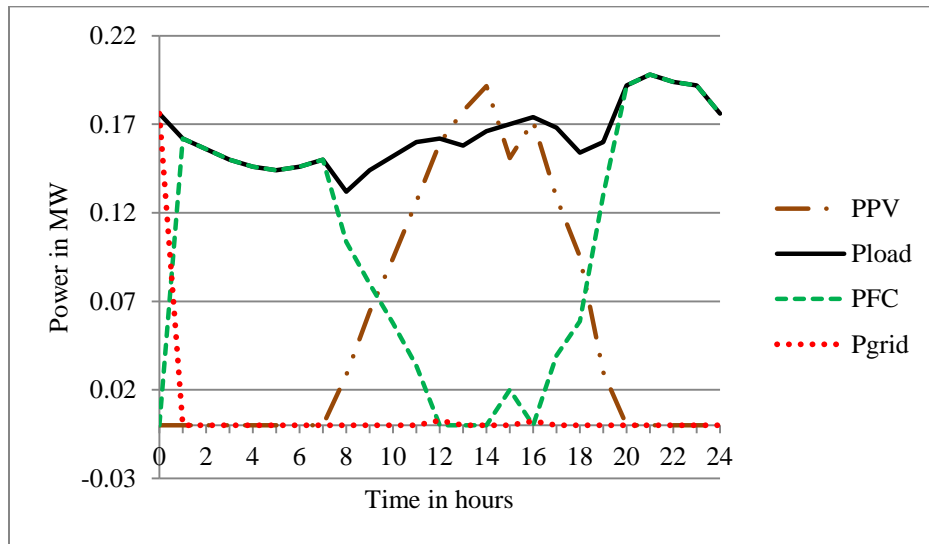
451 **5.4 Analysis of variation of microgrid’s operating cost for different initial SOC levels**
 452 **during start of the day**

453 This section will analyze the variation in the microgrid’s operating cost for different initial SOC
 454 levels during the start of the day. Prior to the analysis, it is necessary that the microgrid’s
 455 operating cost in the absence of battery energy storage, be evaluated. Hence, this section is
 456 divided into two sub-sections, (i) microgrid operation without battery source, and (ii) microgrid
 457 operation with battery source having initial SOC levels at 100%, 70%, and 50% during the start
 458 of the day.

459 **5.4.1 Microgrid operation without battery energy storage**

460 This section discusses the operation of grid connected microgrid without battery source. All the
 461 distributed sources present in the microgrid, including utility grid, should satisfy the forecasted
 462 load demand for the 24h time period. In this case, there may be instances where the output power

463 from the PV may exceed the load demand. Since the battery source is unavailable for charging
464 the excess power, a load resistor is modeled to ground the excess power. By load demand and
465 maximum available power from the distributed sources, the results for the microgrid operation
466 for mix-mode are presented in Fig. 9.



467

468 Fig.9 Optimal operation of microgrid without battery source

469 The total operating cost of the microgrid in this case is \$ 3,332/day. Since there is no battery
470 source available to deliver ancillary service, the maximum available power from the fuel cell and
471 utility grid is drawn by the load. This forces the fuel cell to extend its operating hours by 20h.

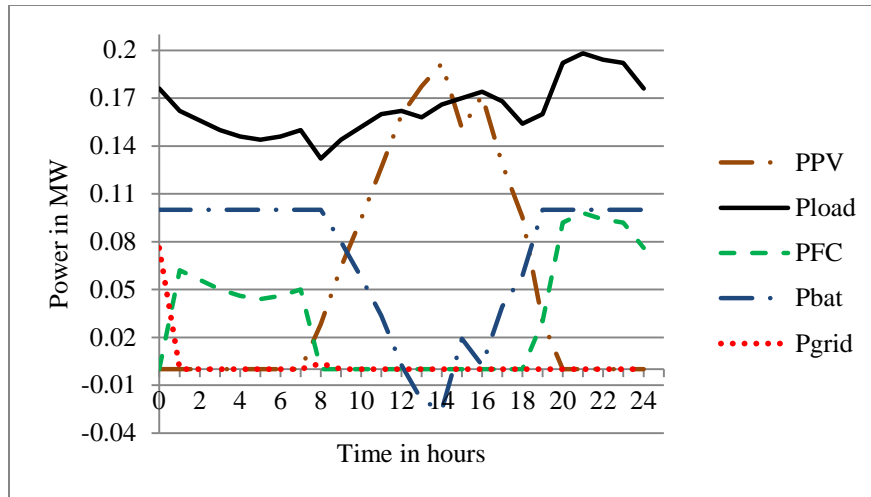
472 Overall, since no battery is employed, the microgrid rely on power from the fuel cell and the
473 utility grid. Furthermore, the fuel cell operating hours exceeds that of the utility grid operating
474 hours. This is because the power drawn from the fuel cell is cheaper than power purchased from
475 the utility grid. There are instances where utility grid is scheduled instead of the fuel cell. During
476 the entire 24h operating time, the utility grid is optimally scheduled for 3h.

477

478

479 **5.4.2 Microgrid operation with battery source having initial SOC levels at 100%, 70% and**
480 **50% during start of the day**

481 The lead-acid battery is added to the microgrid test system for this case study. During the early
482 morning hours, since the battery source is cheap, it will effectively be used to supply the varying
483 load. There is no chance of the battery charging during the early morning hours that is before the
484 sun-rise. Keeping the initial battery cost in mind, the initial SOC of the battery during the start of
485 the day is set to 100%. The results in Fig. 10 portray the optimal dispatch values of the
486 distributed sources in the microgrid when the battery initial SOC level is 100% during the start of
487 the day. The optimal battery capacity for this case is found to be 2,185.4 kWh. During the early
488 morning hours that is before the sun-rise, the power to the load is managed by battery, fuel cell,
489 and the utility grid. During the day, when PV power is present, the battery source is efficiently
490 managed to supply the load or charge when PV power exceeds the load demand. During this
491 period of operation, the power from the fuel cell and utility grid are quite low, or in some cases
492 zero for the majority of the time period. This is due to the availability of cheaper battery power.
493 During the evening hours along the side of battery source the fuel cell is also used to supply the
494 load. The power drawn from the utility grid is zero during this time, because the power purchase
495 cost from the utility grid is very high than the cost of power drawn from battery source and fuel
496 cell. From Fig. 11, it is clear that the battery SOC level is kept within the limits.

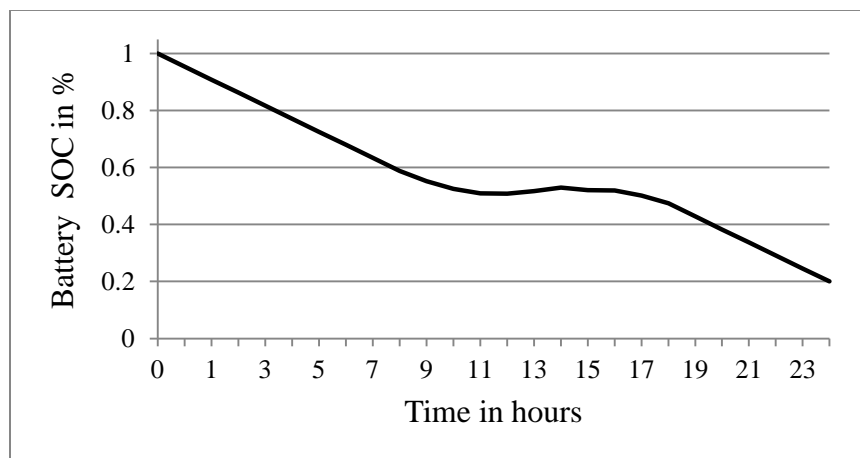


497

498 Fig.10 Optimal output of distributed source in microgrid for when battery initial SOC at 100% of

499

2,185.4 kWh



500

501 Fig.11. Battery SOC level for mix-mode operating strategy when battery initial SOC at 100% of

502

2,185.4 kWh

503 A battery size of 2,185.4 kWh is the optimal capacity when the initial SOC is at 100% during the

504 start of the day. It is our interest to set the initial SOC level to 70% and 50% during the start of

505 the day for the battery size of 2,185.4 kWh and observe the operation of the microgrid and

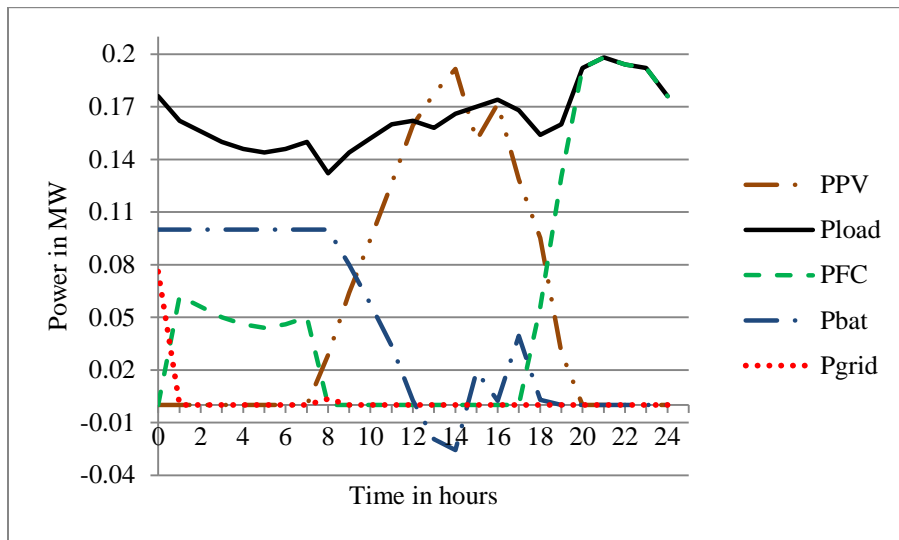
506 calculate its operating cost. Fig. 12 and Fig.13 shows the optimal dispatch values and battery

507 SOC level when the battery initial SOC level is set to 70% of 2,185.4 kWh during the start of the

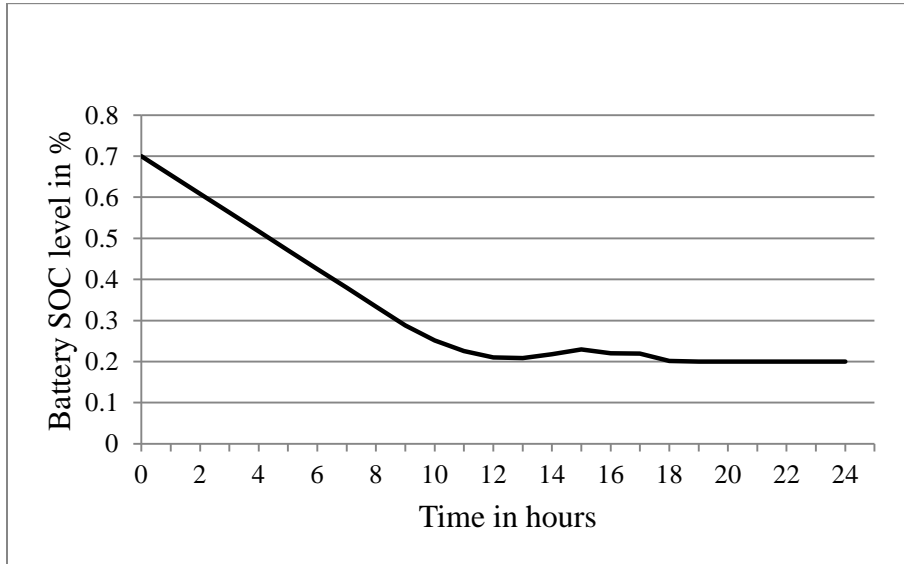
508 day. Similarly, Fig.14 and Fig15 shows the optimal dispatch values and battery SOC level when
509 the battery initial SOC level is set to 50% of 2,185.4 kWh during start of the day.

510 The discharging action of battery in each time step of the day is restricted to how much it charges
511 in previous hours. It can be noticed from Fig.10, Fig.12 and Fig.14 that when the initial SOC is
512 high during the start of the day the battery operates for longer hours. On the other hand, when the
513 initial SOC level of the battery is set low, the battery operating hours is less due to the scarcity of
514 charge in the battery source. When the initial SOC is 70% in Fig.12, the battery operating hours
515 is found to be less, and the battery is completely switched OFF during the night hours. Similarly,
516 when initial SOC is 50% in Fig.14, the battery is switched OFF during night hours and even for
517 few hours during the day-time. For cases of lower initial SOC levels, particularly during night
518 hours, the second unit of the fuel cell is switched ON to supply power to varying load, since the
519 power drawn from utility grid is more expensive. A brief comparison of the microgrid's
520 operating cost without and with battery source with different initial SOC levels are presented in
521 Table.4. The operating cost of the microgrid without battery source is determined to be
522 \$3,332/day. The microgrid operating cost with optimal battery source of 2,185.4 kWh having an
523 initial SOC at 100% at the start of the day is \$ 978.8768/day. This means that operating the
524 microgrid with optimal battery sizing reduces the overall operating cost by 70% for a single day.
525 This is due to the availability of the battery source, and therefore, the battery operating hours is
526 increased to 22h. On the other hand, with the same optimal battery size where the initial SOC is
527 set at 70% during the start of the day, it will reduce the overall operating cost by only 55% for a
528 single day. Moreover, this increases the fuel cell operating hours to 14h, and reduces the battery
529 operating hours to 18h. For an initial SOC of 50% during the start of the day case, the operating
530 cost of the microgrid is \$ 2,335.3/day, where the savings is only 30% for a single day, which is

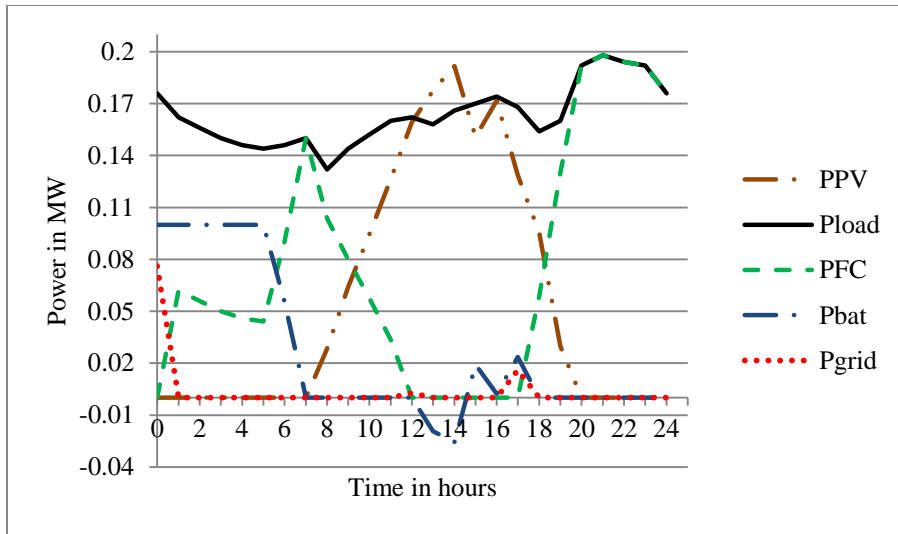
531 even lesser than the higher initial SOC cases. In this case, the fuel cell and utility grid operating
532 hours are increased to 18h and 3h, respectively while the battery run time is reduced to 10h.



533
534 Fig.12 Optimal output of distributed source in microgrid for when battery initial SOC at 70% of
535 2,185.4 kWh



536
537 Fig.13. Battery SOC level for mix-mode operating strategy when battery initial SOC at 70% of
538 2,185.4 kWh

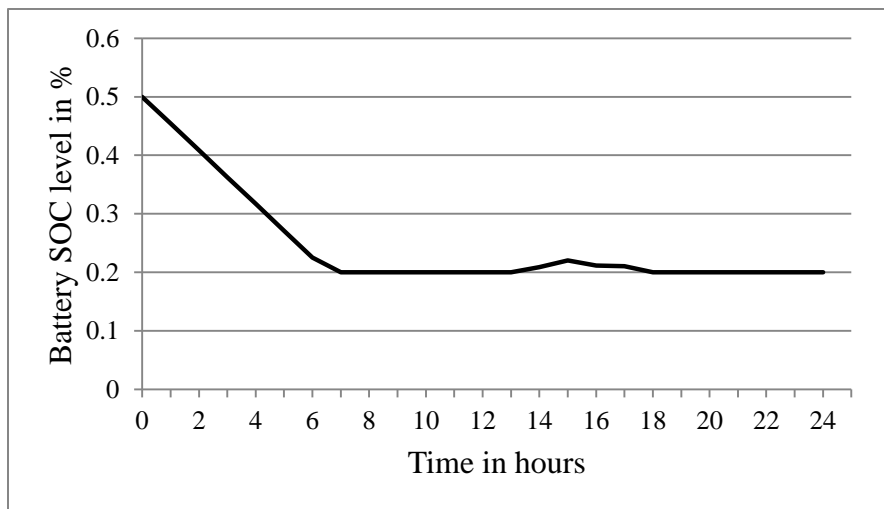


539

540 Fig.14 Optimal output of distributed source in microgrid for when battery initial SOC at 50% of

541

2,185.4 kWh



542

543 Fig.15. Battery SOC level for mix-mode operating strategy when battery initial SOC at 50% of

544

2,185.4 kWh

545

546

547

548

549

Table 4. Comparison of operating cost with and without battery case.

| | With battery source | | | Without battery source |
|--------------------------------|---------------------|-------|---------|------------------------|
| Optimal BES capacity (kWh) | 2185.4 | | | - |
| Battery initial SOC level | 100% | 70% | 50% | - |
| Operating cost in (\$/day) | 978.8768 | 1,491 | 2,335.3 | 3,332 |
| Fuel cell operating (hr) | 13 | 14 | 18 | 20 |
| Grid operating (hr) | 2 | 2 | 3 | 3 |
| Battery operating (hr) | 22 | 18 | 10 | - |
| Savings in operating cost in % | 70% | 55% | 30% | - |

550

551

552 Table 4 shows that if the battery source is optimal with higher initial SOC during the start of the
553 day, there is a significant reduction in microgrid’s operating cost. Moreover, the fuel cell
554 operating hours will also be reduced, which will increase its calendar life. During the microgrid
555 mix-mode operation, the utility grid operating hours is lower as the power purchase cost from the
556 utility grid is very high.

557 From the discussions, it can be concluded that,

558 (i) Operating the microgrid under the proposed mix-mode operating strategy can effectively
559 reduce the its operating cost.

560 (ii) Including battery source in the microgrid will reduce the daily operating cost.

561 (iii) Installing optimal battery capacity with higher initial SOC is highly recommended because
562 the optimal battery capacity with higher initial SOC will reduce the daily operating cost with
563 lowest battery’s capital cost.

564 (iv) Installing battery capacity with higher initial SOC reduces fuel cell and utility grid operating
565 hours.

566 There is no recommendation found in literature on settings of the initial battery SOC level for
567 microgrid operation. Based on the results depicted in Fig.8 and Table 3 it is highly recommended
568 that the battery capacity with higher initial SOC be used during the start of the day. This will

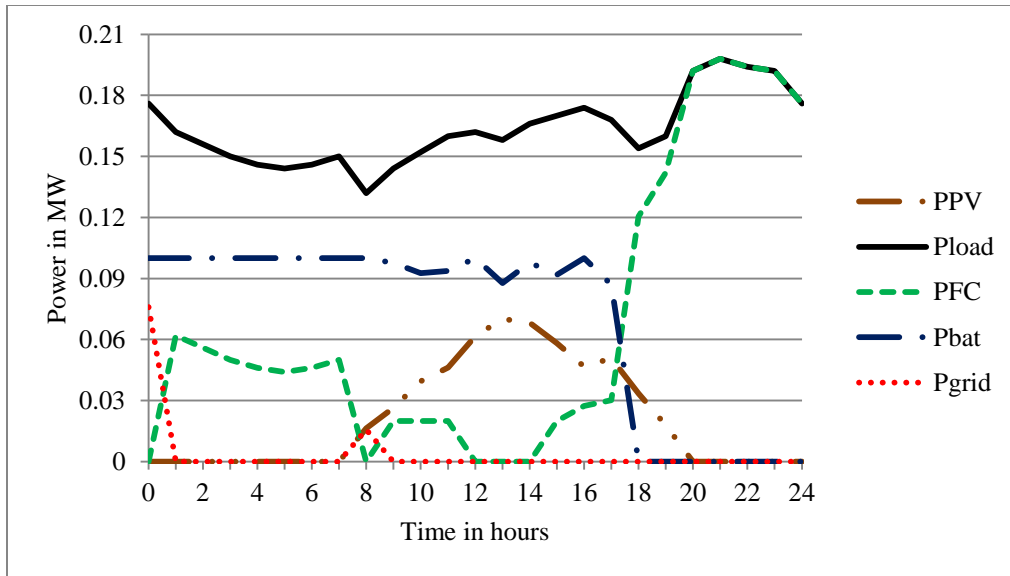
569 reduce the microgrid's operating cost with less battery capital cost, which is the battery's TCPD.
570 When there is no possibility of battery charging during the start of the day's operation, it is
571 highly recommended that the initial SOC of the battery be set to 100%. If there are any possible
572 charging events, then the battery initial SOC can be set to 90% - 95%.

573 **5.5 Analysis on variation of microgrid's operating cost considering uncertainty in PV** 574 **output power**

575 Output power from the solar PV plant is uncertain and relies on solar radiation, which is
576 intermittent in nature. As a result of this, considerable effect in microgrid's operating cost and
577 battery source operation can be found. Therefore, in this section an analysis on variation of
578 microgrid's operating cost and battery source operation is carried out for changes in the PV
579 output power. In this analysis, the energy capacity of the lead-acid battery source, evaluated in
580 Section 5.4.2 for the initial SOC level of 100%, is considered. Hence, the energy capacity of the
581 battery source considered for this analysis is 2,185.4 kWh, and the initial SOC level during the
582 start of the day is set to 100% as recommended in Section 5.4.2.

583 The optimal battery capacity of 2,185.4 kWh is evaluated for a particular PV output power
584 pattern. This analysis is carried out to study the variation of microgrid's operating cost and
585 battery source operation when the PV output power changes. Two PV output power patterns, (i)
586 PV output power from the solar plant during winter and (ii) PV output power from the solar plant
587 during summer are considered for the study.

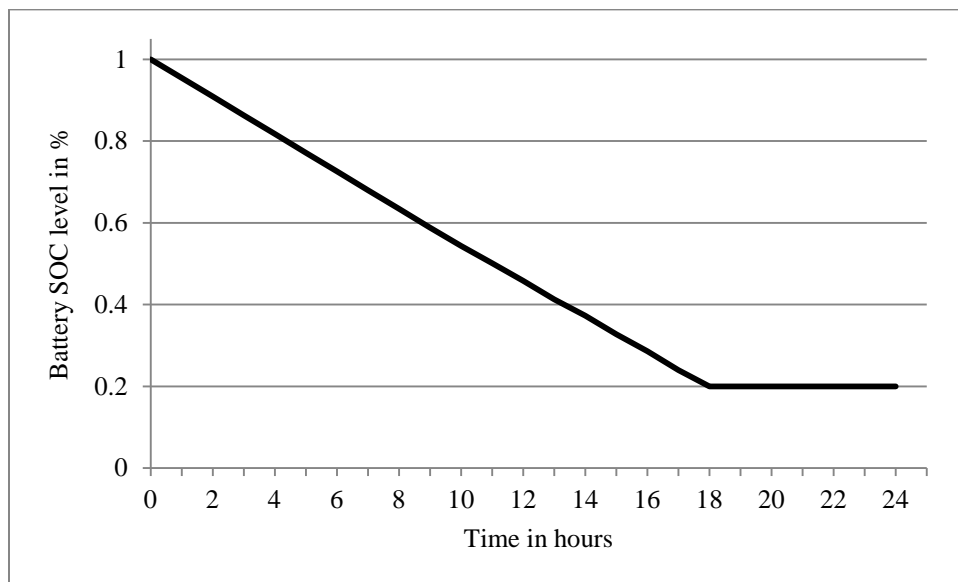
588 Results in Fig.16 shows the optimal dispatch values of the distributed sources in the microgrid
589 for a day in winter, with its corresponding battery SOC level plotted in Fig.17.



590

591

Fig.16 Optimal output of distributed source in microgrid during a day in winter



592

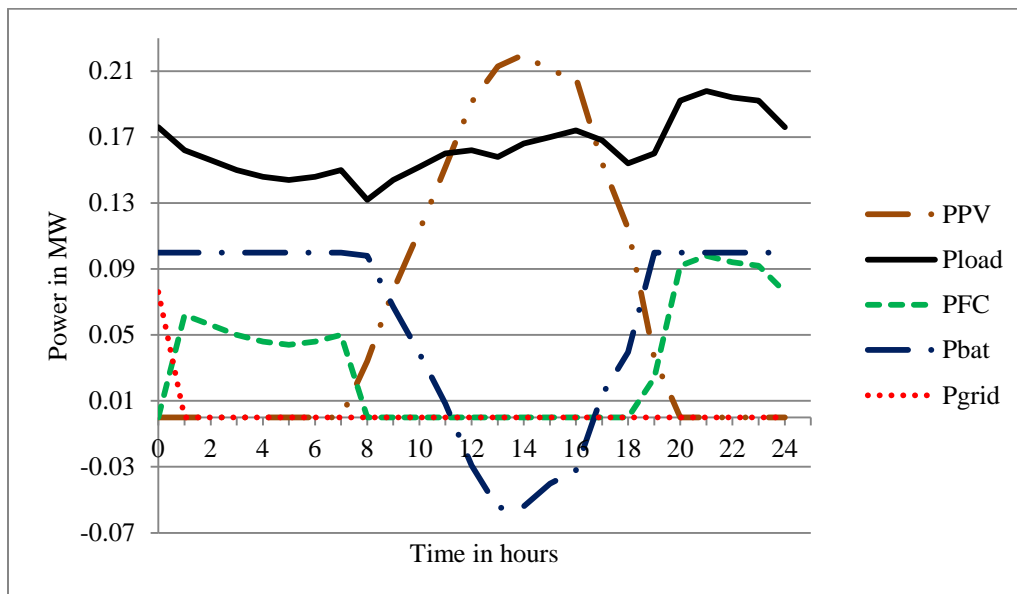
593

Fig.17 Battery SOC level for a day in winter

594 During the early morning hour that is before the sun-rise, the power to the load is managed by
 595 the battery source, fuel cell, and the utility grid. The utility grid is utilized because the power
 596 drawn from the utility grid is cheap in morning hours. During the day hours, the power to the
 597 varying load is managed by PV output power, battery, and fuel cell. Since the PV output power
 598 is less during the winter, the battery source is forced to discharge in-order to manage the load

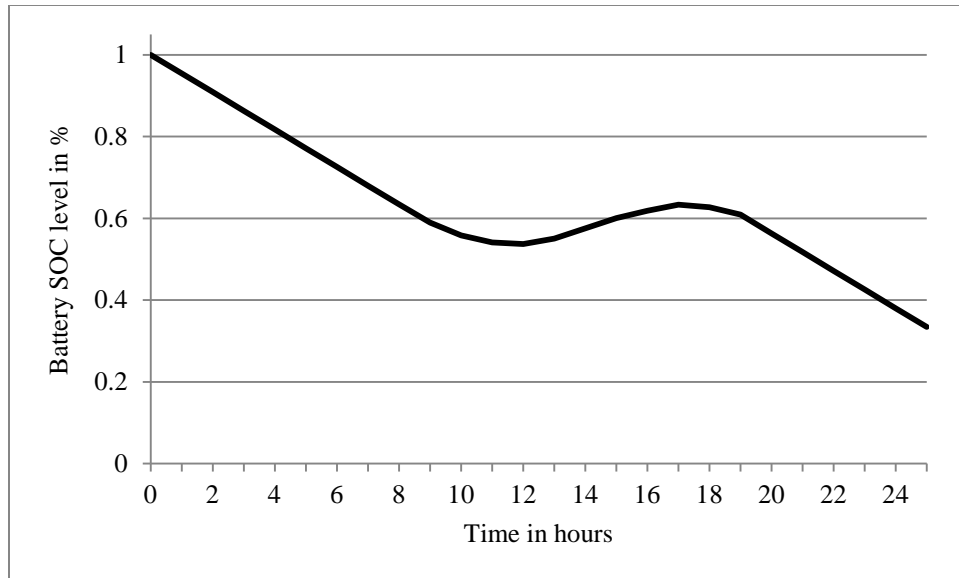
599 demand. It is also evident from Fig.16, that the fuel cell dispatches power for few hours during
 600 the day to manage power to the load demand. During these hours, the power drawn from the
 601 utility grid is kept at zero, considering its cost. Since the power from the battery is cheap, it is
 602 utilized most of the time during the day, and since the PV output power is less than the load,
 603 there are no battery charging instances. During evening hours, the battery power is unavailable
 604 because the SOC level has reached its minimum level due to the fact that the battery source is
 605 effectively utilized during the day hours. Therefore, during evening hours, fuel cell is effectively
 606 utilized to supply power to varying load demand. As a result of this, both the fuel cell units are
 607 switched ON to supply the varying load. The power from the utility grid is kept at zero due to the
 608 cost of power produced from the fuel cell is being less compared to the power drawn from the
 609 utility grid.

610 Fig.18 and Fig.19 are the optimal dispatch values of microgrid's sources and battery SOC level
 611 for a day in summer respectively.



612

613 Fig.18 Optimal output of distributed source in microgrid during a day in summer



614

615

Fig.19 Battery SOC level for a day in summer

616

During the early morning hours, the load demand is supplied by the power from utility grid,

617

battery source, and fuel cell. The utility grid is utilized because the power drawn from the utility

618

grid is cheap during the morning hours. During the day, when PV power is available, the battery

619

source is effectively managed in order to supply power to the load demand. The power from the

620

PV plant is high during the summer, and there are instances where the PV output power

621

exceeded the load demand. As a result of this, during these instances, the battery source operates

622

in the charging mode. During the day, since the availability of the PV power is high, the power

623

drawn from the utility grid and fuel cell is zero, and as a result of this, the fuel cell operating

624

hours is reduced. During the evening hours, the varying load demand is supplied by the battery

625

source and fuel cell. Since the battery source is charged for few hours during the day, it is

626

effectively utilized to supply power during the evening hours. As a result of this, only one fuel

627

cell unit is utilized to manage the load demand. During the evening hours, the power drawn from

628

the utility grid is zero.

629 A comparison on microgrid's operating cost and microgrid sources operating hours are presented
630 in Table 5 for a day for both winter and summer seasons.

631 Table 5. Comparison of microgrid's operating cost and microgrid sources operating hours

| | | |
|----------------------------|-----------|---------|
| Optimal BES capacity (kWh) | 2185.4 | |
| Battery initial SOC level | 100% | |
| | Winter | Summer |
| Operating cost in (\$/day) | 2,413.630 | 925.510 |
| Fuel cell operating (hr) | 20 | 13 |
| Grid operating (hr) | 2 | 1 |
| Battery operating (hr) | 17 | 20 |

632 It can be noticed that the microgrid's operating cost is very much reduced during the day in the
633 summer compared to winter. This is due to the availability of PV power during the day of
634 summer. During the summer, the availability of PV output power is more and the large amount
635 of load demand during the day hours is taken care of by the power from the PV plant.
636 Simultaneously, there are instances of battery charging during the day time when the PV output
637 power exceeded the load demand. As a result of this, the charged battery power is effectively
638 utilized during the evening hours, which reduces the microgrid's operating cost for the day in
639 summer. Due to this reason the battery operating hours is increased to 20h during the day in
640 summer. Since the battery power is available for longer hours, it eventually contributes to the
641 reduction in utility grid and fuel cell operating hours, and the utility grid and fuel cell operates
642 for 1h and 13h, respectively, during the day in summer.

643 On the other hand, the output power from the PV plant is lesser during winter, and the battery
644 source is effectively utilized during the day hours to supply power to the varying load demand.
645 Since the power from the PV plant is lesser than the load demand, there are no charging
646 instances for battery source. As a result of this, the battery source is unavailable during the
647 evening hours. Therefore, the battery source's operating hours is reduced to 17h. In order to

648 supply power to the load during the evening hours, both the units of fuel cell were forced to
649 supply power to the varying load demand. Since the availability of battery source is less in the
650 winter, the fuel cell and utility grid's operating hours increased to 20h and 2h, respectively. As a
651 result of this, the microgrid's operating cost is increased to \$ 2,413.63/day during the day of the
652 winter.

653 **6. Conclusion**

654 In this paper, a mix-mode energy management strategy (MM-EMS) for operating the microgrid
655 at the lowest operating cost and optimal battery sizing method for economic microgrid operation
656 is presented. The mix-mode operating strategy is worked out by solving economic dispatch
657 problem for three proposed strategies, namely continuous run mode, power sharing mode, and
658 ON/OFF mode. Linear programming and mixed integer linear programming optimization
659 techniques were used to solve the energy management problem. With this, a method to find
660 optimal battery size for the microgrid operating under mix-mode strategy was also presented.
661 The battery sizing problem was solved using the PSO optimization technique. The battery's
662 capital cost, its energy and power constraints, and distributed generator's operational limits were
663 taken into account while solving this problem.

664 Compared to other operating strategies, operating the microgrid under mix-mode operating
665 strategy would eventually reduce the microgrid's daily operating cost. Moreover, the proposed
666 battery sizing method was highly accurate in determining the optimal size of battery energy
667 storage for economic operation of the microgrid. The variation of the optimal battery capacity
668 with different sets of initial SOC levels was analyzed, and based on the analysis, it was found
669 that the optimal battery capacity increased as we selected lower initial SOC levels during the
670 start of the day. It was also found that the optimal battery capacity with higher initial SOC level

671 reduced the microgrid's operating cost effectively with lower battery initial cost. Furthermore,
672 variation to the microgrid's operating cost against different SOC levels was analyzed. It was
673 found that as the initial SOC level during the start of the day was reduced, a significant reduction
674 in savings in the microgrid's operating cost became evident. Based on the results, a
675 recommendation on the choice of initial SOC level during the start of the day for an economical
676 operation of a microgrid was suggested. Finally, an analysis on variation of microgrid's
677 operating cost considering uncertainty in PV output power was carried out. It was found that the
678 availability of PV power from solar photovoltaic plant influenced the microgrid's operating cost
679 and battery source's operation.

680 **Acknowledgements**

681 This work is supported by the Ministry of Education, Malaysia under High Impact Research
682 Grant (HIR-MOHED000004-16001).

683 **References**

- 684 [1] S. Shivashankar, S. Mekhilef, H. Mokhlis, M. Karimi. Mitigating methods of power
685 fluctuation of photovoltaic (PV) sources—A review. *Renewable and Sustainable Energy Reviews*
686 2016; 59:1170-84.
- 687 [2] S. Koochi-Kamali, N. Rahim, H. Mokhlis. Smart power management algorithm in microgrid
688 consisting of photovoltaic, diesel, and battery storage plants considering variations in sunlight,
689 temperature, and load. *Energy Conversion and Management* 2014; 84:562-82.
- 690 [3] C. Chen, S. Duan, T. Cai, B. Liu, G. Hu. Smart energy management system for optimal
691 microgrid economic operation. *IET Renewable Power Generation* 2011; 5:258-67.
- 692 [4] F.A. Mohamed, H.N. Koivo. Multiobjective optimization using Mesh Adaptive Direct Search
693 for power dispatch problem of microgrid. *International Journal of Electrical Power & Energy*
694 *Systems* 2012; 42:728-35.
- 695 [5] F.A. Mohamed, H.N. Koivo. System modelling and online optimal management of microgrid
696 using mesh adaptive direct search. *International Journal of Electrical Power & Energy Systems*
697 2010; 32:398-407.
- 698 [6] D. Tenfen, E.C. Finardi. A mixed integer linear programming model for the energy
699 management problem of microgrids. *Electric Power Systems Research* 2015; 122:19-28.
- 700 [7] H. Khodr, N. El Halabi, M. García-Gracia. Intelligent renewable microgrid scheduling
701 controlled by a virtual power producer: a laboratory experience. *Renewable energy* 2012;
702 48:269-75.

703 [8] Xiongwen Zhang, Siew-Chong Tan, Guojun Li, Zhenping Feng. Components sizing of
704 hybrid energy systems via the optimization of power dispatch simulations. *Energy* 2013; 52:165-
705 172.

706 [9] Y.-S. Cheng, M.-T. Chuang, Y.-H. Liu, S.-C. Wang, Z.-Z. Yang. A particle swarm
707 optimization based power dispatch algorithm with roulette wheel re-distribution mechanism for
708 equality constraint. *Renewable energy* 2016; 88:58-72.

709 [10] M. Kalantar. Dynamic behavior of a stand-alone hybrid power generation system of wind
710 turbine, microturbine, solar array and battery storage. *Applied Energy* 2010; 87:3051-64.

711 [11] S. Mousavi G. An autonomous hybrid energy system of wind/tidal/microturbine/battery
712 storage. *International Journal of Electrical Power and Energy Systems* 2012; 43:1144-54.

713 [12] S. Berrazouane, K. Mohammedi. Parameter optimization via cuckoo optimization algorithm
714 of fuzzy controller for energy management of a hybrid power system. *Energy Conversion and*
715 *Management* 2014; 78:652-60.

716 [13] S. Chen, H.B. Gooi, M. Wang. Sizing of energy storage for microgrids. *IEEE Transactions*
717 *on Smart Grid* 2012; 3:142-51.

718 [14] B. Bahmani-Firouzi, R. Azizipanah-Abarghooee. Optimal sizing of battery energy storage
719 for micro-grid operation management using a new improved bat algorithm. *International Journal*
720 *of Electrical Power & Energy Systems* 2014; 56:42-54.

721 [15] J.P. Fossati, A. Galarza, A. Martín-Villate, L. Fontán. A method for optimal sizing energy
722 storage systems for microgrids. *Renewable energy* 2015; 77:539-49.

723 [16] C. Chen, S. Duan, T. Cai, B. Liu, G. Hu. Optimal allocation and economic analysis of
724 energy storage system in microgrids. *IEEE Transactions on Power Electronics* 2011; 26:2762-73.

725 [17] S. Sharma, S. Bhattacharjee, A. Bhattacharya. Grey wolf optimisation for optimal sizing of
726 battery energy storage device to minimise operation cost of microgrid. *IET Generation,*
727 *Transmission & Distribution* 2016; 10:625-637.

728 [18] Y. Li, S. Rajakaruna, S. Choi. Control of a solid oxide fuel cell power plant in a grid-
729 connected system. *IEEE Transactions on Energy Conversion* 2007; 22:405-13.

730 [19] X. Wang, B. Huang, T. Chen. Data-driven predictive control for solid oxide fuel cells.
731 *Journal of Process Control* 2007; 17:103-14.

732 [20] K.A. Pruitt, R.J. Braun, A.M. Newman. Establishing conditions for the economic viability
733 of fuel cell-based, combined heat and power distributed generation systems. *Applied Energy*
734 2013; 111:904-20.

735 [21] X. Tan, Q. Li, H. Wang. Advances and trends of energy storage technology in Microgrid.
736 *International Journal of Electrical Power & Energy Systems* 2013; 44:179-91.

737 [22] W. Gu, Z. Wu, R. Bo, W. Liu, G. Zhou, W. Chen, et al. Modeling, planning and optimal
738 energy management of combined cooling, heating and power microgrid: A review. *International*
739 *Journal of Electrical Power & Energy Systems* 2014; 54:26-37.

740 [23] W. Al-Saedi, S.W. Lachowicz, D. Habibi, O. Bass. Power quality enhancement in
741 autonomous microgrid operation using particle swarm optimization. *International Journal of*
742 *Electrical Power & Energy Systems* 2012; 42:139-49.

743 [24] Chee Wei Tan, Tim C.Green, Carlos A. Hernandez-Aramburo. A stochastic method for
744 battery sizing with uninterruptible-power and demand shift capabilities in PV (photovoltaic)
745 systems. *Energy* 2010; 35:5082-5092.

746
747